Bio-Design and Manufacturing (2024) 7:399–412
https://doi.org/10.1007/s42242-024-00299-x

RESEARCH ARTICLE

A drug-loaded flexible substrate improves the performance of conformal cortical electrodes

Rongrong Qin[1] · Tian Li[1] · Yifu Tan[1] · Fanqi Sun[2,3] · Yuhao Zhou[2,3] · Ronghao Lv[1] · Xiaoli You[2,3] · Bowen Ji[2,3] · Peng Li[1] · Wei Huang[1,4]

Received: 10 January 2024 / Accepted: 30 May 2024 / Published online: 12 July 2024

Abstract

Cortical electrodes are a powerful tool for the stimulation and/or recording of electrical activity in the nervous system. However, the inevitable wound caused by surgical implantation of electrodes presents bacterial infection and inflammatory reaction risks associated with foreign body exposure. Moreover, inflammation of the wound area can dramatically worsen in response to bacterial infection. These consequences can not only lead to the failure of cortical electrode implantation but also threaten the lives of patients. Herein, we prepared a hydrogel made of bacterial cellulose (BC), a flexible substrate for cortical electrodes, and further loaded antibiotic tetracycline (TC) and the anti-inflammatory drug dexamethasone (DEX) onto it. The encapsulated drugs can be released from the BC hydrogel and effectively inhibit the growth of Gram-negative and Gram-positive bacteria. Next, therapeutic cortical electrodes were developed by integrating the drug-loaded BC hydrogel and nine-channel serpentine arrays; these were used to record electrocorticography (ECoG) signals in a rat model. Due to the controlled release of TC and DEX from the BC hydrogel substrate, therapeutic cortical electrodes can alleviate or prevent symptoms associated with the bacterial infection and inflammation of brain tissue. This approach facilitates the development of drug delivery electrodes for resolving complications caused by implantable electrodes.

Rongrong Qin and Tian Li have contributed equally to this work.

✉ Bowen Ji
bwji@nwpu.edu.cn

✉ Peng Li
iampli@nwpu.edu.cn

✉ Wei Huang
vc@nwpu.edu.cn

[1] Frontiers Science Center for Flexible Electronics (FSCFE), Xi'an Institute of Flexible Electronics (IFE) and Xi'an Institute of Biomedical Materials & Engineering (IBME), Northwestern Polytechnical University, Xi'an 710072, China

[2] Unmanned System Research Institute, Northwestern Polytechnical University, Xi'an 710072, China

[3] Ministry of Education Key Laboratory of Micro and Nano Systems for Aerospace, School of Mechanical Engineering, Northwestern Polytechnical University, Xi'an 710072, China

[4] Key Laboratory of Flexible Electronics of Zhejiang Province, Ningbo Institute of Northwestern Polytechnical University, Ningbo 315103, China

Graphic abstract

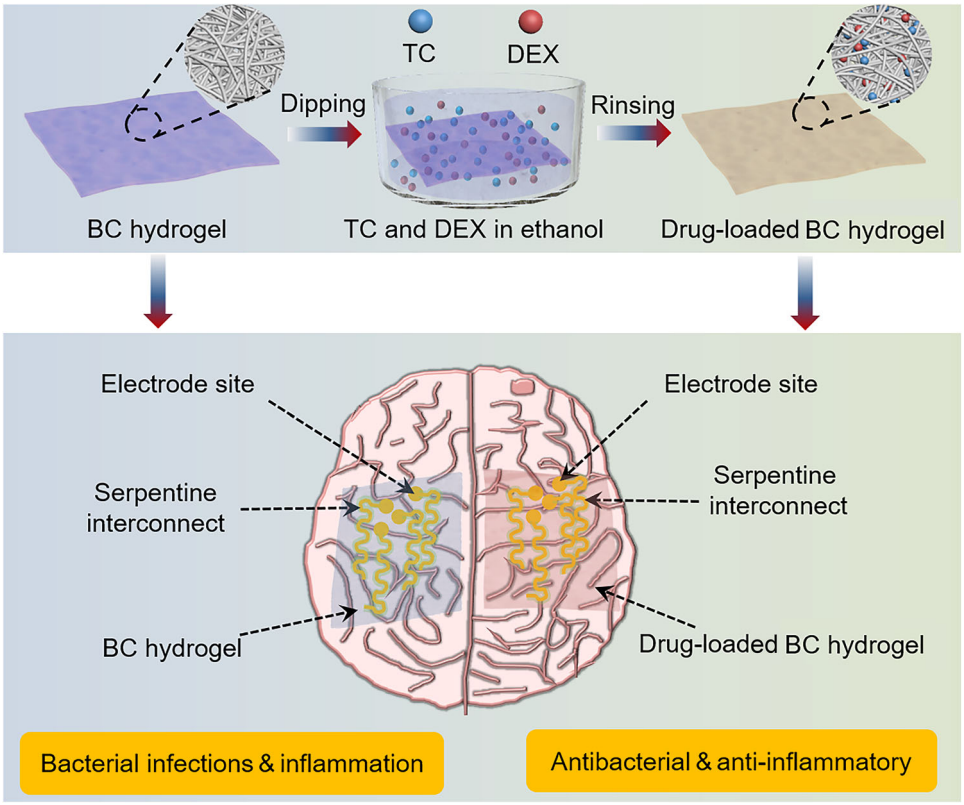

Keywords Antibacterial · Anti-inflammatory · Drug loading · Cortical electrodes · Bacterial cellulose hydrogel

Introduction

Cortical electrodes are important tools for neuroscience research, since they enable the recording of brain activity [1, 2], stimulate neural networks [3, 4], and work in tandem with optogenetics [5]. In general, cortical electrodes must facilitate the stable recording of neural signals in the body over time. However, cortical electrodes, since they are implantable foreign bodies, are also known to trigger inflammatory reactions [6–8]. Moreover, the wounds caused by surgical implantation of electrodes are associated with a risk of bacterial infection [7], and some estimates of surgical site infection rates are as high as 20%. Bacterial infections can also further exacerbate inflammatory reactions, thereby inducing swelling and loss of function of the tissue. Taken together, these consequences can erode the quality and bandwidth of signals across the body–electrode interface. Moreover, once a craniocerebral infection occurs, electrodes need to be removed to avoid secondary injury, resulting in failed implantation [8].

Flexible cortical electrodes (usually composed of polyimide (PI), polycarbonate (PC), or a polydimethylsiloxane (PDMS)-based insulating substrate) have recently become an attractive alternative to conventional rigid electrodes [9, 10]. However, given the intrinsic dissimilarities between soft, wet, and living biological tissues and impermeable, dry, and synthetic substrate materials [11], these electrodes may not fully conform to three-dimensional (3D) neural tissues since they can trigger immune responses, gliosis, and neuronal degeneration after implantation [12, 13]. Therefore, there is a critical need to develop conformal cortical electrodes that show a higher degree of compatibility with soft brain tissue. Since they are natural materials, bacterial cellulose (BC) hydrogels have mechanical properties that are similar to biological tissues. This is because they have a porous structure that contains a large percentage of water, which resembles the structure of the tissue extracellular matrix [14]. BC hydrogels also have outstanding properties regarding softness, surface porosity, optical transparency, and biocompatibility, and therefore have been widely used in biomedical engineering [15, 16], drug delivery [17, 18], and functional electric devices [19, 20].

To develop antibacterial and anti-inflammatory cortical electrodes, we prepared a functional BC hydrogel by loading tetracycline (TC) [21, 22] and dexamethasone (DEX) [23, 24] into the hydrogel itself. TC is an antibiotic used to treat and prevent infectious disease and has a wide antibacterial spectrum against Gram-positive and Gram-negative bacteria, including spirochetes, actinomycetes, and mycoplasma. DEX is a corticosteroid that can significantly inhibit the foreign body response, thereby reducing the inflammatory reaction. The encapsulation and controlled release of drugs by the BC hydrogel are regulated by the porous network formed by the close-packing of cellulose, which generates a structure with pore diameters in the 10–100 nm range [25, 26]. Therapeutic cortical electrodes were then developed by integrating drug-loaded BC hydrogel with serpentine-shaped Parylene-C arrays; these were then used for recording high-resolution electrocorticography (ECoG) signals in a rat model. Therapeutic cortical electrodes with serpentine structures that consist of both periodic arcs and straight segments can offer high levels of stretchability that can facilitate electrode application. Moreover, because of the controlled release of TC and DEX from the BC hydrogel substrate, it is hoped that the use of therapeutic cortical electrodes can greatly alleviate bacterial infection and inflammation. These results demonstrate the potential of therapeutic cortical electrodes for resolving the complications caused by implantable neural electrodes.

Materials and methods

Materials

BC was purchased from Hainan Yide Food Co., Ltd. (China). TC and DEX were purchased from Shanghai Titan Technology Co., Ltd. (China). Phosphate-buffered saline (PBS) was purchased from Beijing Solarbio Science & Technology Co., Ltd. (China). Artificial cerebrospinal fluid (ACSF) was purchased from Shanghai Yuanye Biotechnology Co., Ltd. (China). Ecoflex gel, which cures at room temperature (73 °F/23 °C) and shows negligible shrinkage, was purchased from Smooth-On, Inc. (USA).

Methods

Preparation of drug-loaded BC hydrogels

The BC hydrogel used here is produced by the fermentation of *Acetobacter xylinum* (ATCC53582). It has a purity of >95% and a solid content of approximately 15%. We first cut the untreated BC hydrogel into 5 cm×5 cm squares, and then added them to a 0.1 mol/L sodium hydroxide solution. This was boiled at 100 °C for 15 min to remove attached cell fragments and culture medium components. The hydrogel was then transferred into deionized water at room temperature until the solution was no longer alkaline. Finally, the BC hydrogel was dried in a drying oven at 45 °C for 24 h and then stored in a drying cabinet.

Next, we prepared a solution containing a mixture of different concentrations of TC and DEX dissolved in ethanol. Specifically, we generated solutions in which the concentration of DEX was 5 mg/mL and the concentration of TC was 1, 2, or 3 mg/mL. The pretreated BC was then immersed in one of the above three concentration solutions and mixed by stirring in the dark for 24 h for drug loading. Residual drug on the BC surface was then quickly washed with ethanol, and drug-loaded hydrogels were then dried in a drying oven at 45 °C. After drying, loaded hydrogels were stored in a refrigerator at 4 °C in the dark for later use. We named the drug-loaded BC hydrogels BC-DEX/TC-1, BC-DEX/TC-2, and BC-DEX/TC-3 based on the concentration of TC present in the mixed solution.

Preparation of conformal therapeutic cortical electrodes

Next, nine-channel serpentine arrays were fabricated using micro electro mechanical system (MEMS) processes. The main fabrication processes involved were as follows. First, a four-inch silicon wafer was rinsed using the standard Radio Corporation of America (RCA) cleaning method, which was released in 1970 by Kern and Puotincn of RCA. A 300-nm-thick aluminum (Al) sacrificial layer was evaporated on the wafer using electron beam evaporation coating equipment (WF1DEGN01, Denton, USA), which facilitates the release of flexible electrodes from the wafer. A 3-μm-thick Parylene-C layer was deposited by chemical vapor (PDS2010 system, Specialty Coating Systems, USA), and a 200-nm-thick layer of Au was subsequently sputtered by a magnetron sputtering coating system (WF1DMSP01, Denton, USA). The serpentine pattern of the Au layer was first photolithographed, and then a layer of Parylene-C was deposited. Reactive ion etching was then used to remove Parylene-C from excess and electrode sites. The retained patterned Parylene-C was then used as the encapsulation layer of the serpentine Au layer to complete electrode preparation.

To release the arrays from the wafer, the wafer was first covered by three layers of airlaid paper and a four-inch glass wafer, and two clips were used to clamp the stacked wafers along their edges. These were then immersed in 20% HCl solution for 24 h to finish the slow process of metal sacrifice (Al), and then rinsed in deionized water before being fully dried for 2 h in a 100 °C oven while in the clamping state. After releasing the clips, water-soluble adhesive tape (polyvinyl alcohol, PVA, Aquasol, North Tonawanda, USA) was used to easily retrieve the Parylene-C electrodes from the silicon wafer.

Finally, the nine-channel arrays were transferred to BC and BC-DEX/TC-2 hydrogels coated with Ecoflex gel. The Ecoflex gel was then cured at room temperature to bond the electrode arrays to the BC or BC-DEX/TC-2 hydrogel. The electrodes were then soaked in water to remove water-soluble tape and expose the electrode site. The electrode pad and wire were then connected by a hot press to complete the preparation of BC- and BC-DEX/TC-2-based cortical electrodes.

Morphology characterization

We observed the surface morphology of natural raw BC and drug-loaded BC (i.e., BC-DEX/TC-1, BC-DEX/TC-2, and BC-DEX/TC-3) hydrogels via scanning electron microscopy (SEM, Gemini 300, ZEISS, Germany). Here all samples were first prepared by freeze-drying. We used atomic force microscopy (AFM, Dimension Icon, Bruker, USA) in the standard tapping mode to measure the surface roughness of BC and drug-loaded BC hydrogels.

Fourier transform infrared spectroscopy

Attenuated total reflectance Fourier transform infrared (ATR-FTIR) spectroscopy (Tensor II, Bruker, USA) was performed in transmission mode with a scan range of 400–4000 cm^{-1} and a resolution of 4 cm^{-1}.

Element analysis

Since N is an element specific to TC and F is an element specific to DEX, we confirmed whether the drug was loaded in BC hydrogel by X-ray photoelectron spectroscopy (XPS) (Kratos AXIS Ultra DLD, KRATOS, Japan). The binding energy was calibrated by setting the C 1s peak at 284.6 eV. An energy-dispersive spectrometer (EDS) was used to analyze whether the encapsulated drug was evenly distributed throughout the BC hydrogel.

Average loading density of TC and DEX in the drug-loaded BC hydrogels

Since TC and DEX can be dissolved in ethanol, the quantity of TC and DEX loaded in the functionalized BC hydrogel was determined by immersing functionalized BC hydrogels (1 cm $\times$1 cm) in 2000 μL ethanol under shaking at 37 °C at a speed of 100 r/min. During release experiments, 500 μL aliquots of the release solution was pipetted out at 12-h intervals, and 500 μL fresh ethanol was then added to the release samples. Since TC and DEX present in the functionalized BC hydrogel could be completely dissolved in ethanol, the equilibrium cumulative release amount is the loading capacity of TC and DEX loaded onto the BC hydrogel. Accordingly, the absorbances of TC and DEX were measured in the wavelength range from 200 to 450 nm using an ultraviolet–visible (UV–Vis) spectrophotometer (U-3900H, Hitachi, Japan). The experiment was carried out using five or more technical replicates.

Water contact angle analysis

The wettability of the BC, BC-DEX/TC-1, BC-DEX/TC-2, and BC-DEX/TC-3 hydrogels was evaluated using a water contact angle analysis system (DSA25, KRUSS, Germany). All measurements were performed using deionized water with a drop size of 2 μL. To improve testing reliability, three to five technical replicates were obtained for each sample.

Thermogravimetric analysis

We performed thermogravimetric analysis (TGA) measurements for both raw BC and drug-loaded BC hydrogels using a Pyris 1 thermogravimetric analyzer (PerkinElmer Instruments, China). Hydrogel degradation was investigated over a range from 25 to 600 °C at a heating rate of 10 °C/min.

In vitro drug-release testing

Next, in vitro drug-release testing was performed by immersing functionalized BC hydrogels (1 cm$\times$1 cm) in 1000 μL PBS or ACSF and shaking at 37 °C at a speed of 100 r/min. During release experiments, 500 μL aliquots of release solution was obtained after 0.5, 1, 2, 4, 8, 12, 24, 36, 48, and 72 h, and 500 μL PBS or ACSF was then added to release samples. The TC and DEX contents were then measured using the method mentioned above.

In vitro antimicrobial performance of the drug-loaded BC hydrogel

Standard agar plating method Original bacterial (i.e., *Staphylococcus aureus* (*S. aureus*) or *Escherichia coli* (*E. coli*)) solutions were diluted with Mueller–Hinton broth (MHB) to a concentration of 1×10^7 CFU/mL (CFU: colony-forming units). Prepared dry BC, BC-DEX/TC-1, BC-DEX/TC-2, and BC-DEX/TC-3 hydrogel squares of 1 cm$\times$ 1 cm were then placed into sterile 24-well plates. Three technical replicates were used for each material, and no sample in the well plate was used as a control group. Bacterial droplets (50 μL) were then added to the sample surface and incubated at 37 °C at a humidity of approximately 90% for 4 h. Next, 450 μL PBS buffer solution was added to resuspend bacteria on the sample surface. Well plates containing samples were then treated ultrasonically for 3 min so that bacteria that adhered to the surface of the hydrogel could be resuspended in PBS. Next, 100 μL of the resuspended solution was transferred to new 96-well plates for tenfold gradient dilution.

Diluted bacterial solution (50 μL) was then inoculated onto an agar plate, and CFUs were counted after incubation at 37 °C overnight. The antimicrobial reduction formula is as follows:

$$\log\ \text{Reduction} = \log \frac{\text{Cell count of control}}{\text{Survivor count on sample}}.$$

In addition, 50 μL of the suspension after 1000-fold dilution was spread on the agar plate and incubated at 37 °C for 16 h.

Bacterial morphology Bacteria (1×10^7 CFU/mL) were inoculated on 1 cm×1 cm squares of dry BC, BC-DEX/TC-1, BC-DEX/TC-2, and BC-DEX/TC-3 hydrogels, and then incubated at 37 °C for 4 h. Samples were then fixed with 4% paraformaldehyde for 1 h and subsequently dehydrated using gradient ethanol solutions. Finally, dried samples were coated with gold before SEM observation.

In vitro biological safety testing

The in vitro biological safety of BC and BC-DEX/TC-2 hydrogels was evaluated using cell viability and hemocompatibility tests. These processes are described as follows:

Cell viability testing NIH 3T3 cells were first seeded at a density of 10,000 per well in a well plate, and then incubated at 37 °C with 5% CO_2. After 24 h, cells that adhered to the plate wall were observed under a microscope. Next, the cell culture medium (which contained Dulbecco's modified eagle medium (DMEM), newborn calf serum (NBCS), penicillin sulfate, and streptomycin) was aspirated, and BC and BC-DEX/TC-2 hydrogels were placed onto a plate. After that, 500 μL of cell culture medium was added to each well and incubated at 37 °C with 5% CO_2 to allow the material to interact with the cells. After 24 h, the culture medium of each well was aspirated, and the BC and BC-DEX/TC-2 hydrogels were removed. The residual medium in the cell plate was then washed with PBS. A detection reagent containing Alamar Blue diluted with cell culture medium (volume fraction: 1/9) was then added to the plate. After incubation for 4–6 h in a dark environment, 100 μL of detection reagent was transferred to a new 96-well plate. The fluorescence density value of each sample at 590 nm was measured using a BioTek Synergy Neo2 system. The formula used to calculate cell viability was as follows:

$$\text{Cell viability} = \frac{F_{\text{expt.}}}{F_{\text{ctrl.}}} \times 100\%,$$

where $F_{\text{expt.}}$ represents the fluorescence density of the hydrogels and $F_{\text{ctrl.}}$ represents the fluorescence density of the control group (i.e., the cell culture medium).

In addition, after each sample was incubated with NIH 3T3 for 1 d, the live–dead cell staining reagent was added and co-incubated with the sample for another 20 min. Cell survival status was then observed by fluorescence microscopy (EVOS FL Auto 2, Thermal Fisher Scientific, USA).

Hemocompatibility testing Here, we measured the hemolysis activity of the samples using fresh New Zealand rabbit blood. Briefly, 1 cm×1 cm squares of BC and BC-DEX/TC-2 hydrogels were first transferred into Eppendorf (EP) tubes. Tris-NaCl buffer was then set as a negative control and 0.1% (volume fraction) Triton X-100 was set as a positive control. Next, 500 μL of an erythrocyte suspension was added to each EP tube and incubated at 37 °C for 1 h. Sample absorbance at 540 nm was then measured using a UV–Vis spectrophotometer. The formula used to calculate the hemolytic ratio is as follows:

$$\text{Hemolytic ratio} = \frac{A_{\text{sample}} - A_{\text{negative}}}{A_{\text{positive}} - A_{\text{negative}}} \times 100\%,$$

where A_{sample} is the absorbance of the groups treated with BC and BC-DEX/TC-2, A_{positive} and A_{negative} are the absorbances of the positive (i.e., 0.1% Triton X-100) and the negative (i.e., Tris-NaCl buffer) controls, respectively.

Animal experiments

In this study, a Sprague–Dawley male rat (290 g) was anesthetized with isoflurane and fixed in a stereotaxic frame. A rectangular craniotomy was performed using a surgical drill, and the bone flap was separated with a microdissector, leaving the cerebral dura mater exposed. A cranial window of approximately 4 mm×3 mm in size was made by exposing the area across the somatomotor and somatosensory cortices. A stainless-steel screw electrode was then implanted in the drill holes, with a reference position placed in the cerebellum, which exhibits lower activity than other brain sites. *S. aureus* (10 μL) solution (1×10^7 CFU/mL) was then inoculated onto the BC-based and BC-DEX/TC-2-based cortical electrodes. The BC-based and BC-DEX/TC-2-based electrodes were closely adhered to the left and right cortical surfaces of the rat brain to record the ECoG signals, respectively. ECoG signals from nine channels were then amplified and digitized at a sampling rate of 1 kHz using a multichannel acquisition processor (Plexon Inc., USA). All data were processed using an EEGLAB package with a frequency pass band of 0.5–200 Hz.

In vivo antibacterial testing

After electrode implantation for 3 d, the rat was anesthetized by intraperitoneal injection of pelltobarbitalum Natricum

(100 mg/kg) and then perfused transcardially with 4% paraformaldehyde in PBS. After removal of the skin and skull, a part of the brain was fixed in 4% formaldehyde overnight before being sectioned into 100-μm-thick sections for subsequent histological analysis. The part of the brain tissue that was in contact with the electrodes was removed and ultrasonically cleaned in 1 mL PBS for 30 min, and then a solution containing PBS and bacteria was inoculated on agar plates. These plates were then incubated at 37 °C for 24 h to count the number of colonies.

Immunofluorescence staining

For immunofluorescence staining, sections were stained with neuronal nuclei antigen (NeuN) for neurons, glial fibrillary acidic protein (GFAP) for astrocytes, and 4′,6-diamidino-2-phenylindole (DAPI) for nuclei. Subsequently, sections were observed with laser confocal microscopy. We analyzed the intensity of the astrocyte reaction by using ImageJ to measure the relative fluorescence intensity of astrocytes in brain tissue sites in contact with BC-based and BC-DEX/TC-2-based cortical electrodes. Fluorescence intensity was obtained by measuring the brightness of the pixel areas at the electrode–brain interface relative to tissues 3 mm beneath the interface.

Inflammatory cytokine detection

Next, we examined the expression levels of inflammatory cytokines such as interleukin-1β (IL-1β), tumor necrosis factor-α (TNF-α), interleukin-10 (IL-10), and transforming growth factor-β (TGF-β) to evaluate the anti-inflammatory performance of the BC-DEX/TC-2-based electrodes. TNF-α and IL-1β were used as key proinflammatory markers, and IL-10 and TGF-β were used as key anti-inflammatory markers. Semiquantitative analysis was performed on tissue sections using Aipathwell software to calculate the histochemical score (H-Score) of each inflammatory factor for the analyzed brain tissue sections. The H-Score is a commonly used metric to characterize immunohistochemical analyses, and converts the number of positive cells in each section and their staining intensity into values to achieve semiquantitative tissue staining. H-Score ranges from 0 to 300, and the larger the number, the stronger the comprehensive positive intensity.

Results and discussion

Successful construction of drug-loaded BC hydrogels

The one-pot encapsulation of TC and DEX in the BC hydrogel was initiated by immersing preprocessed BC into a mixed solution containing specific concentrations of TC and DEX dissolved in ethanol. Here, we used a DEX concentration of 5 mg/mL and a TC concentration of 1, 2, and 3 mg/mL, respectively (Fig. 1a). Due to the abundance of pores in BC and the action of osmotic pressure, the solvent exchanges with the water held in BC, and can then drugs enter and adsorb into the BC fiber network. The resultant drug-loaded BC hydrogels were named BC-DEX/TC-1, BC-DEX/TC-2, and BC-DEX/TC-3 based on the concentration of TC originally present in the mixed solution. The amount of TC and DEX drugs that were successfully loaded was determined by XPS since N is specific to TC, and F is specific to DEX (Fig. 1b). The characteristic peaks of TC at 1510 cm^{-1} and DEX at 1607 cm^{-1} in the ATR-FTIR spectra of the drug-loaded BC hydrogels further demonstrated the successful loading of TC and DEX (Fig. 1c). The encapsulation densities of TC and DEX in the BC hydrogel increased with higher drug feed concentrations (Fig. 1d and Fig. S1 in Supplementary Information). Moreover, EDS images showed that the encapsulated drug was evenly distributed in the hydrogel (Fig. 1e and Fig. S2 in Supplementary Information). This result was also verified by SEM and AFM images (Figs. 1f and 1g; Figs. S3 and S4 in Supplementary Information). We observed no obvious differences in surface morphology between the BC and the drug-loaded BC hydrogels, indicating that not only the drug distribution was uniform, but also that the drug-loading process had no influence on hydrogel structure.

Basic performance and controlled release behavior of drug-loaded BC hydrogels

Since the drug was distributed uniformly, even when packed with functional molecules the drug-loaded BC hydrogels maintained a certain degree of optical transparency (Fig. 2a). The light transmissivity of the wet BC-DEX/TC-1 hydrogel was about 60%–90% between 420 and 800 nm. However, when the amount of drug loaded onto the hydrogel increased, the transmittance of the wet BC-DEX/TC-2 and wet BC-DEX/TC-3 hydrogels decreased to about 40%–70% between 420 and 800 nm (Fig. 2b). The transparency of drug-loaded hydrogels used as electrode substrates is beneficial for locating interface sites in vivo and for observing morphological changes in tissues beneath electrodes. As shown in Fig. 2c, the drug-loaded BC hydrogels were more hydrophilic than the BC hydrogel. Excellent hydrophilicity is known to be of great significance for the conformal attachment of electrodes to brain tissue and for maintaining high electrode biocompatibility during implantation [27]. Since the manufacturing processes for therapeutic cortical electrodes involve high-temperature treatments such as hot pressing for connecting the electrode pad and wire, at which the temperature can reach 220 °C [28], the thermal stability of the BC hydrogel is also crucial. As shown by the thermogravimetric (TG)

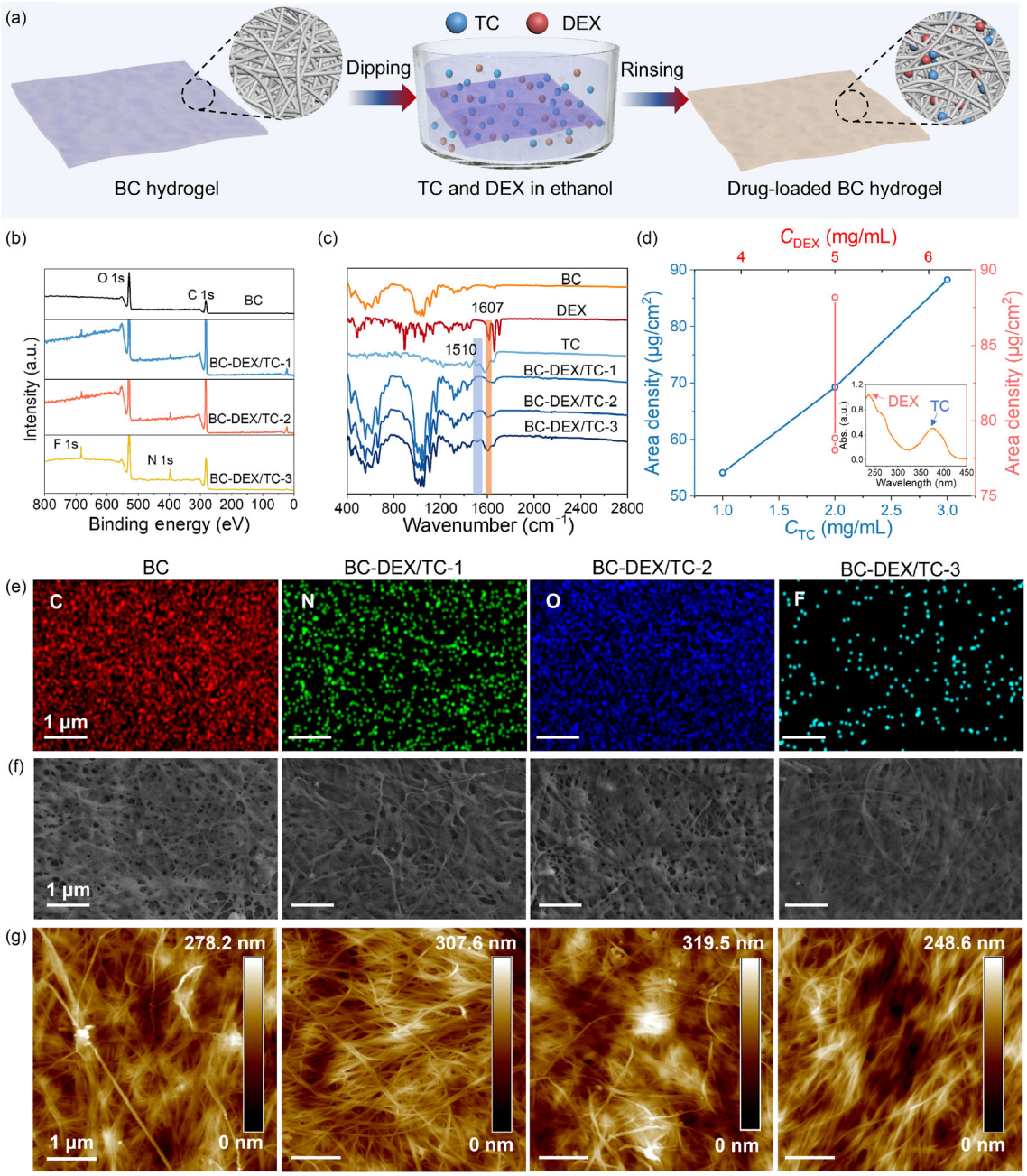

Fig. 1 **a** Illustration of the drug-loaded BC hydrogel fabrication process. **b** XPS specta of the BC, BC-DEX/TC-1, BC-DEX/TC-2, and BC-DEX/TC-3 hydrogels. **c** FTIR spectra of the BC, DEX, TC, BC-DEX/TC-1, BC-DEX/TC-2, and BC-DEX/TC-3 hydrogels. **d** Experimental loading density of the BC-DEX/TC-1, BC-DEX/TC-2, and BC-DEX/TC-3 hydrogels at different TC and constant DEX feeding doses. The inserted panel shows the classic UV absorption curve of the two drugs released from BC-DEX/TC in ethanol. **e** EDS spectra of the BC, BC-DEX/TC-1, BC-DEX/TC-2, and BC-DEX/TC-3 hydrogels. **f** SEM morphological characterization of the BC, BC-DEX/TC-1, BC-DEX/TC-2, and BC-DEX/TC-3 hydrogels. **g** AFM images of the BC, BC-DEX/TC-1, BC-DEX/TC-2, and BC-DEX/TC-3 hydrogels. BC: bacterial cellulose; XPS: X-ray photoelectron spectroscopy; DEX: dexamethasone; TC: tetracycline; FTIR: Fourier transform infrared; UV: ultraviolet; EDS: energy-dispersive spectrometer; SEM: scanning electron microscopy; AFM: atomic force microscopy

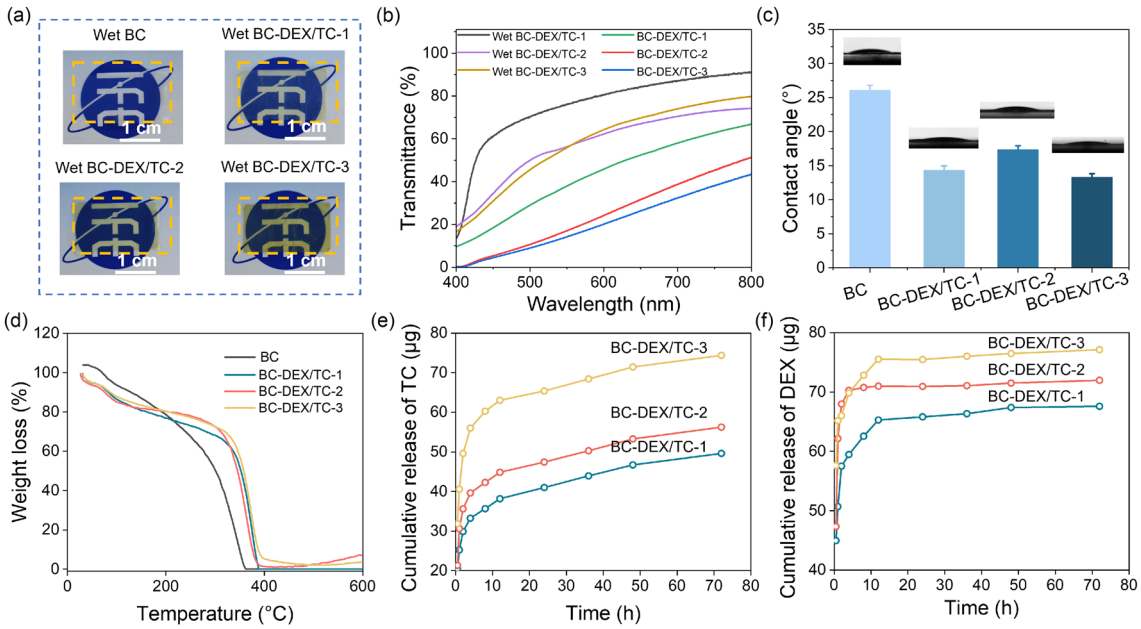

Fig. 2 **a** Transparency of wet BC, BC-DEX/TC-1, BC-DEX/TC-2, and BC-DEX/TC-3 hydrogels. **b** Light transmittance of dry and wet BC-DEX/TC-1, BC-DEX/TC-2, and BC-DEX/TC-3 hydrogels. **c** Water contact angle of the BC, BC-DEX/TC-1, BC-DEX/TC-2, and BC-DEX/TC-3 hydrogels (data are expressed as mean±standard deviation, n=3–5). **d** Thermogravimetric analysis of the BC, BC-DEX/TC-1, BC-DEX/TC-2, and BC-DEX/TC-3 hydrogels from 25 to 600 °C. **e** Cumulative release curve of TC from the BC-DEX/TC-1, BC-DEX/TC-2, and BC-DEX/TC-3 hydrogels in ACSF. **f** Cumulative release curve of DEX from the BC-DEX/TC-1, BC-DEX/TC-2, and BC-DEX/TC-3 hydrogels in ACSF. BC: bacterial cellulose; DEX: dexamethasone; TC: tetracycline; ACSF: artificial cerebrospinal fluid

curves (Fig. 2d), a mass loss (10% in total, mass fraction) due to moisture evaporation from internal adsorbed water was observed from room temperature until 100 °C (i.e., the boiling point of water at normal pressure). After 100 °C, continued weight loss may be attributed to the bound water in the hydrogel. Decomposition was then identified above 300 °C to show a notable weight loss due to the decomposition of organic components. This temperature is much higher than the highest temperature (220 °C) used in the Au–BC manufacturing process.

Since the molecular sizes of TC and DEX are approximately 1.8 nm (Fig. S5 in Supplementary Information), entrapped drugs can then be slowly released from the BC hydrogel via pores formed by closely arranged fibers. Next, to evaluate the drug-release performance from drug-loaded BC hydrogels, we monitored the release behaviors of TC and DEX in ACSF and PBS, respectively. The release profiles of TC and DEX in ACSF are shown in Figs. 2e and 2f as well as Fig. S6 (Supplementary Information). All specimens tested displayed a steady release of the drug after an initial burst release. This release rate and the corresponding equilibrium concentration at a stable plateau varied depending on the initial loading mass of the drugs. The short initial burst may be due to the drug adsorbed on the surface of the drug-loaded BC hydrogels, while the long-term sustained release was due to the drug trapped inside the BC hydrogel. Although the molecular sizes of TC and DEX are nearly identical, and the loading densities of TC and DEX were similar (i.e., 70 and 78 μg/cm^2, respectively), the release rate of DEX was higher than that of TC from the drug-loaded BC hydrogels. This phenomenon is due to the different charges of TC and DEX. The BC matrix is negatively charged, and TC is positively charged, whereas DEX is electrically neutral; TC is therefore released more slowly than DEX due to electrostatic interactions between BC and TC. In addition, drug release from drug-loaded BC hydrogels was faster in PBS than in ACSF, and drug release was essentially complete after 24 h (Fig. S7 in Supplementary Information). Thus, our results show that the drug-loaded BC hydrogels can significantly slow the release rate of both TC and DEX, indicating that the BC hydrogel can be used for slow drug release, thereby reducing the risk of bacterial infection and inflammation during electrode implantation.

In vitro biological performance of the drug-loaded BC hydrogels

TC has a broad antibacterial spectrum that includes Gram-negative and Gram-positive bacteria. In this study, the antibacterial activity of drug-loaded BC hydrogels was investigated using *E. coli* and *S. aureus* as model bacteria. The

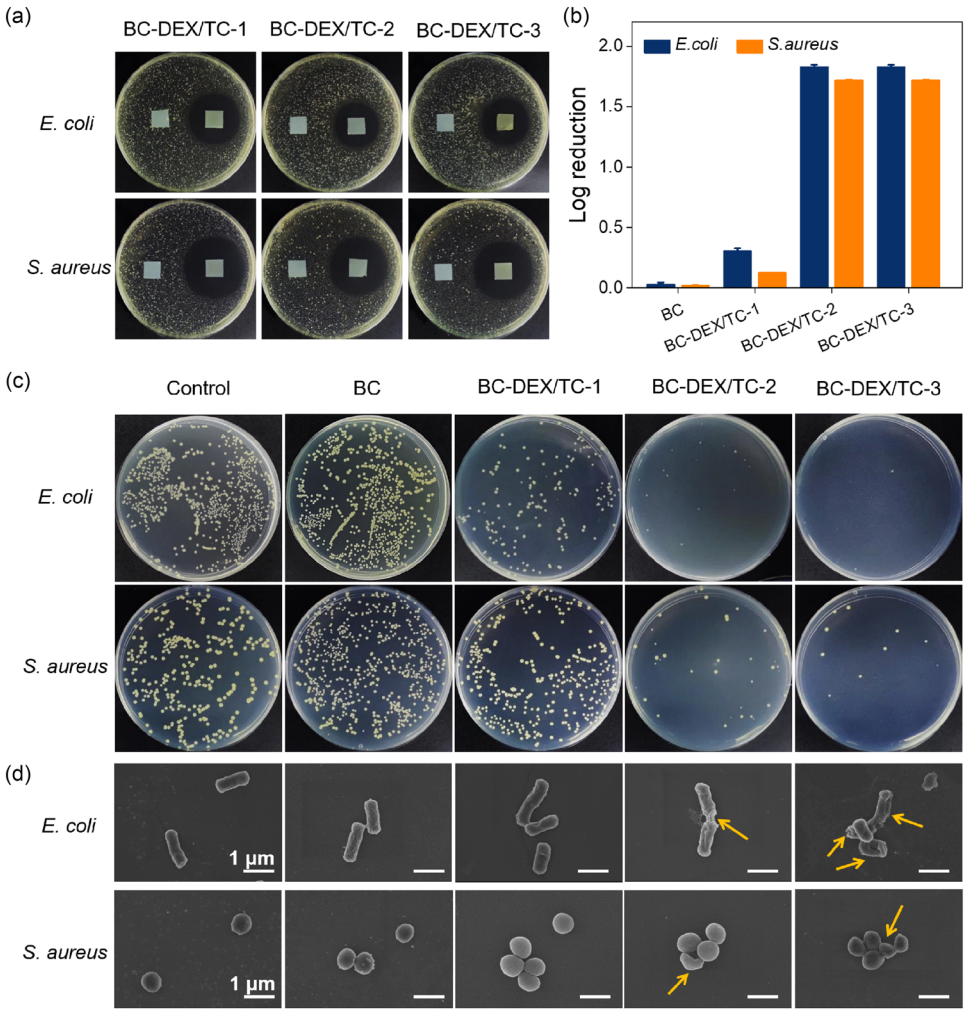

Fig. 3 **a** Bacteriostatic zone of the BC, BC-DEX/TC-1, BC-DEX/TC-2, and BC-DEX/TC-3 hydrogels against *E. coli* and *S. aureus*. **b** In vitro bactericidal activity of the BC, BC-DEX/TC-1, BC-DEX/TC-2, and BC-DEX/TC-3 hydrogels against *E. coli* and *S. aureus* (data are expressed as mean±standard deviation, n=5). **c** Colonies formed by bacteria coated on agar plating after incubation with the BC, BC-DEX/TC-1, BC-DEX/TC-2, and BC-DEX/TC-3. **d** SEM images of *E. coli* and *S. aureus* after coincubation with the BC, BC-DEX/TC-1, BC-DEX/TC-2, and BC-DEX/TC-3 hydrogels. BC: bacterial cellulose; DEX: dexamethasone; TC: tetracycline; SEM: scanning electron microscopy

antibacterial activities of BC and drug-loaded BC hydrogels were investigated using disk diffusion and standard agar plating methods. For example, the prepared hydrogels were placed on agar coated with *E. coli* and *S. aureus*. Antibacterial activity was measured by the generation of a clear zone of inhibition around samples after 24 h of incubation, and these images are shown in Fig. 3a. As expected, no inhibition zones were observed for the BC hydrogel, implying that the BC hydrogel did not exert any antibacterial effect against either of the two tested strains. Next, we observed that the diameters of the zones of inhibition of the BC-DEX/TC-1, BC-DEX/TC-2, and BC-DEX/TC-3 hydrogels against the same bacteria were almost identical (i.e., 3 cm for *E. coli* and 3.5 cm for *S. aureus*). These results indicate that drug-loaded BC hydrogels show strong antibacterial activity.

In addition to the disk diffusion method, antibacterial activity was further evaluated using bacterial growth inhibition assays. Figures 3b and 3c show the numbers of surviving bacteria after 4 h of incubation at 37 °C of a bacterial suspension with different drug-loaded BC hydrogel samples; here survival is shown as a function of TC concentration. We found that all drug-loaded BC hydrogels inhibited bacterial growth, and that bacterial inhibition increased quickly for the samples treated with drug-loaded BC hydrogels, even when only a small amount of TC was loaded onto the BC hydrogel. However, bacterial inhibition leveled off when the TC loading is further increased. The calculated antibacterial ratios showed that BC-DEX/TC-2 and BC-DEX/TC-3 showed nearly identical antibacterial growth activity and performed the best among all samples tested. Specifically, BC-DEX/TC-2 and BC-DEX/TC-3 reduced *E. coli* growth by 1.823±0.021 (> (98.50±4.80)%) and *S. aureus* growth by 1.716±0.007 (> (98.08±1.56)%).

Moreover, we then used SEM to observe the morphological changes in bacteria after different treatments to elucidate the antibacterial mechanisms responsible. After coincubation of BC-DEX/TC-2 and BC-DEX/TC-3 with bacteria, the cell envelopes of the bacteria were seriously destroyed, showing obvious deformation, collapse, and wrinkles, as indicated by the orange arrows in Fig. 3d. In general, these results

indicate that BC-DEX/TC-2 and BC-DEX/TC-3 exert strong antibacterial activity against both Gram-negative *E. coli* and Gram-positive *S. aureus*. We then selected BC-DEX/TC-2, which has a smaller drug load, for further experiments.

Cellular growth and proliferation on surfaces are a symbol of material cytocompatibility, and can therefore be used to assess their potential for application in vivo. Accordingly, cytotoxicity studies were conducted to investigate the effect of BC-DEX/TC-2 on the proliferation of NIH 3T3 cell lines. The effect of BC without drugs was evaluated in vitro to ensure that BC did not exert an independent toxicity effect. The good biocompatibility of BC-DEX/TC-2 was evidenced by the Alamar Blue assay of NIH 3T3. In general, cell viability values greater than 90% were observed after the culturing of NIH 3T3 for 24 h on 24-well plates with different samples, including BC and BC-DEX/TC-2 (Fig. 4a). Fluorescence microscopy was further used to visually evaluate NIH 3T3 viability after coincubation with samples for 24 h. This showed that the number of dead cells was negligible and that NIH 3T3 maintained high viability (Fig. 4b).

Moreover, a hemolysis ratio test was carried out to evaluate the blood compatibility of the BC-DEX/TC-2 hydrogel, which is an important biomedical parameter for assessing the safety of implantable devices. The hemolysis ratios of the BC and BC-DEX/TC-2 hydrogels are shown in Fig. 4c, and the corresponding images are shown in Fig. 4d. Neither the BC hydrogel nor the BC-DEX/TC-2 hydrogel was found to damage human erythrocytes. These results demonstrate the very high biocompatibility of the BC-DEX/TC-2 hydrogel, which implies that it may perform well during implantation assays. The BC-DEX/TC-2 hydrogel, which is highly hydrophilic and as soft as native tissue, is a desirable substrate material for preparing electrodes for neural interfacing.

Conformal therapeutic cortical electrode design and in vivo recording performance

Therapeutic cortical electrodes were prepared by integrating the BC-DEX/TC-2 hydrogel with serpentine-shaped Parylene-C arrays. The resulting electrodes were used to record the ECoG signals of the rat (Figs. 5a and 5b). The serpentine-shaped Parylene-C arrays, which contain nine channels were fabricated using traditional micromachining (Fig. 5c). The minimum metal line width for conducting is 25 μm, the Parylene-C line width for encapsulation is 50 μm, and the diameter of nine exposed microelectrode sites is 100 μm with a pitch of 700 μm between the two adjacent sites (Fig. 5d and Fig. S8 in Supplementary Information). This optimal spacing of arrays has been identified by previous works as capable of achieving relatively high resolution [28].

After release from the silicon wafer, Parylene-C-encapsulated serpentine interconnects were bonded to BC or BC-DEX/TC-2 hydrogel via a sticky silicone adhesive such as Ecoflex gel. The corresponding images of the BC-based or BC-DEX/TC-2-based electrodes are shown in Figs. 5e and 5f. Due to its relatively high softness and hydrophilicity, the BC-based electrode achieves conformal adhesion on the surface of the curved hydrogel (Fig. 5g). The successful adhesion onto the surface of wet material indicates that the electrode can also achieve conformal adhesion onto the surface of the cerebral cortex during implantation, which will help the electrode acquire high-quality ECoG signals. Next, the BC-based and BC-DEX/TC-2-based electrodes were implanted into a rat cerebral cortex to evaluate their recording performance during implantation. The corresponding images are shown in Fig. 5h. We found that the ECoG activity of the rat brain as recorded by multichannel mapping using the BC-based and BC-DEX/TC-2-based electrodes demonstrated the high-throughput signal readout ability of both electrodes (Fig. 5i).

In vivo antibacterial and anti-inflammatory performance of therapeutic cortical electrodes

Next, the drug-release behavior of the therapeutic cortical electrodes was tested in vitro. These results showed that the drug release rate was lower than the rate of a bare BC control due to the adhesive Ecoflex gel layer present between the drug-loaded BC hydrogel and the electrode array. The release time of DEX can be extended from 24 to 150 h, and that of TC can be extended to approximately 350 h (Fig. 6a). Before implantation of BC-based and BC-DEX/TC-2-based electrodes into the rat cerebral cortex, 10 μL *S. aureus* solution (1×10^7 CFU/mL) was added to the electrodes to evaluate the antibacterial and anti-inflammatory performance of the electrodes. After three days of implantation, the brain tissue in contact with the BC-based electrode presented a deeper, more purple-red color relative to the tissue in contact with the BC-DEX/TC-2-based electrode, which is a classic symptom of an inflamed and traumatic infection (Fig. 6b, inserted photograph). Figure 6b and Fig. S9 (Supplementary Information) show the number of surviving bacteria in brain tissue contacted with electrodes after three days of electrode implantation. Here, we see that the BC-DEX/TC-2-based electrode is able to effectively inhibit bacterial growth. For example, the bactericidal rate of the therapeutic cortical electrode was up to 95% compared with the BC-based electrode. Furthermore, the brain tissue sections after hematoxylin–eosin (H&E) staining showed that the structure of the brain in the BC-DEX/TC-2 group was clearer and more complete compared with similar measurements taken in the BC group (Fig. 6c). Taken together, these results show the therapeutic efficacy of BC-DEX/TC-2 electrodes in inhibiting bacterial growth and brain tissue inflammation.

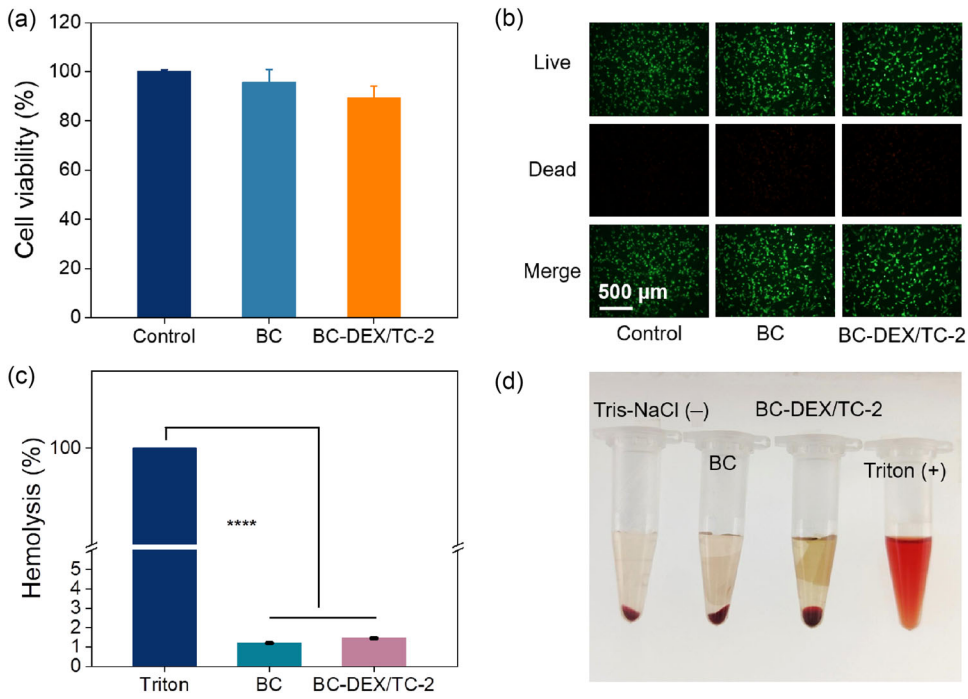

Fig. 4 **a** Viability of NIH 3T3 cells after coincubation with BC and BC-DEX/TC-2 hydrogels for 1 d (data are expressed as mean ±standard deviation, n=5). **b** Fluorescent images showing live (green)/dead (red) NIH 3T3 cells after coincubation with BC and BC-DEX/TC-2 hydrogels for 24 h. **c** Hemolysis ratio of BC and BC-DEX/TC-2 hydrogels (data are expressed as mean±standard deviation, n=5, $^{****}p<0.0001$). **d** Photographs of fresh rabbit blood samples incubated with the BC and BC-DEX/TC-2 hydrogels. BC: bacterial cellulose; DEX: dexamethasone; TC: tetracycline

Next, we examined the accumulation and proliferation of astrocytes in the central nervous system, which can also be regarded as an inflammatory response. To do so, brain tissue was stained by NeuN and GFAP to identify neurons and astrocytes, respectively (Fig. 6d), and the fluorescence intensities of NeuN and GFAP were quantified using ImageJ. These results showed that the GFAP levels of BC-DEX/TC-2-based electrode groups were lower than those of BC-based electrode groups, whereas their NeuN levels were slightly higher (Fig. 6e).

Furthermore, the expression levels of inflammatory cytokines such as IL-1β, TNF-α, IL-10, and TGF-β can be used to evaluate the anti-inflammatory performance of BC-DEX/TC-2-based electrodes. Here, TNF-α and IL-1β were treated as proinflammatory markers, while IL-10 and TGF-β were treated as anti-inflammatory markers. As reflected by the H-Score (histochemical score) of each inflammatory factor in the brain tissue section in contact with the BC-based electrode and the BC-DEX/TC-2-based electrode (Figs. 6f and 6g; Fig. S10 in Supplementary Information), we found that the BC-DEX/TC-2-based electrode was associated with decreased expression of proinflammatory factors and increased expression of anti-inflammatory factors. Taken together, these results demonstrate that BC-DEX/TC-2-based electrodes have good biocompatibility, as well as better antibacterial and anti-inflammatory performance compared to BC-based electrodes.

Conclusions

BC is a naturally produced material whose biocompatibility and softness are superior to those of other synthetic flexible polymers, including PDMS, PI, PC, and Parylene-C. The porous network formed by the close-packed cellulose enables BC hydrogels to be a suitable platform for the encapsulation of functional molecules. In this study, the encapsulated antibiotic TC and anti-inflammatory drug DEX showed sustained release from a BC hydrogel and effectively inhibited the in vitro growth of Gram-negative bacteria *E. coli* as well as the Gram-positive bacteria *S. aureus*. Conformal therapeutic cortical electrodes prepared by integrating drug-loaded BC hydrogels with serpentine-shaped arrays were shown to be able to produce high-resolution ECoG signal recordings using a rat model. Moreover, this system showed efficacy in alleviating in vivo bacterial infection and inflammation caused by the surgical implantation of cortical electrodes. For example, the bactericidal rate of the therapeutic cortical electrode was up to 95% compared with the BC-based electrode. The development of novel therapeutic cortical electrodes by integrating drug-loaded BC hydrogels provides new opportunities for resolving complications caused by implantable flexible electronic devices.

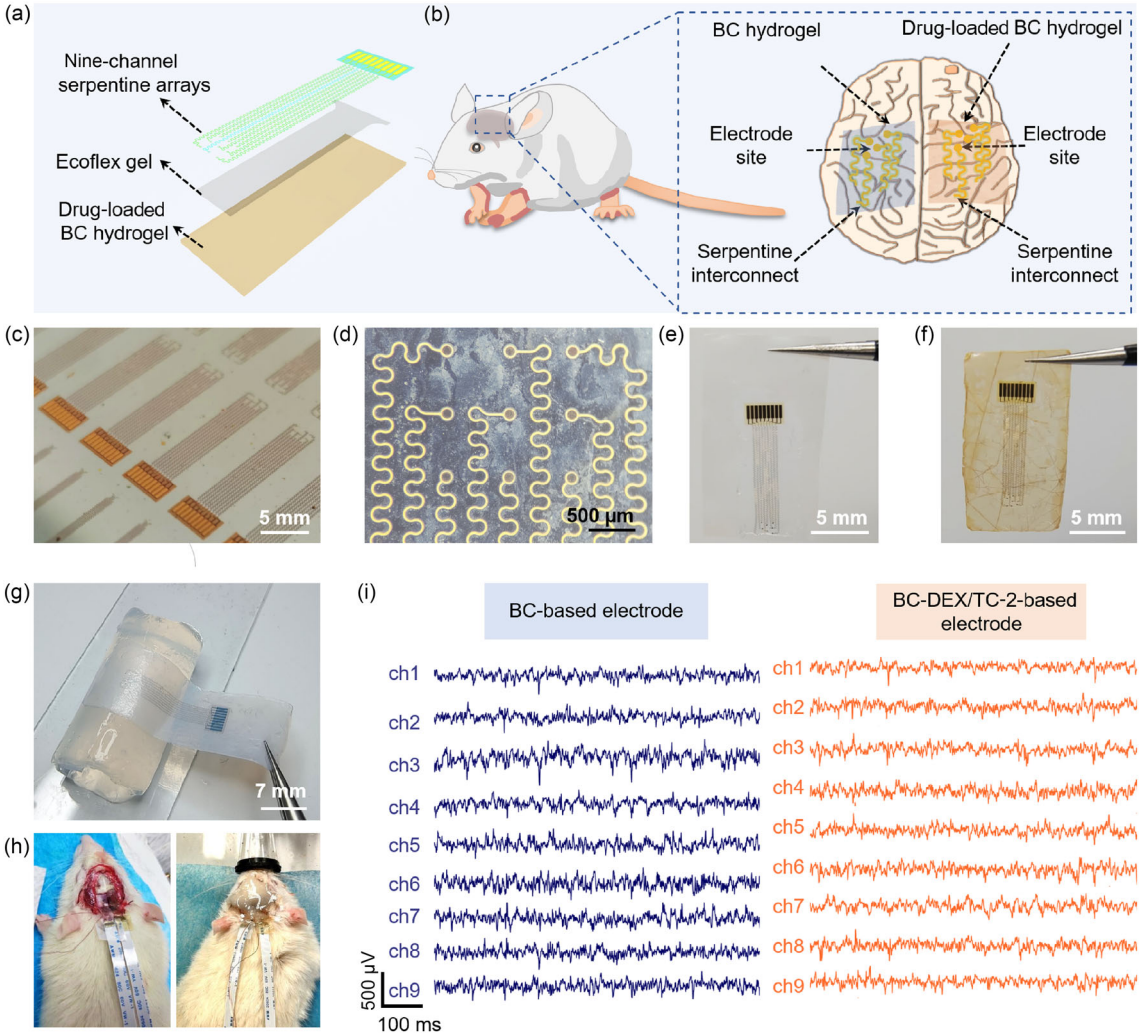

Fig. 5 **a** Layout of proposed therapeutic cortical electrodes. **b** Illustrations of therapeutic cortical electrodes implanted on the rat brain cortex. **c** Photograph of nine-channel serpentine arrays on the silicon wafer. **d** Photograph of a single nine-channel serpentine array following release from the silicon wafer. Photographs of **e** BC-based and **f** BC-DEX/TC-2-based hydrogel cortical electrodes. **g** Photograph of BC-based cortical electrodes attached to the curved surface of an agarose hydrogel. **h** Photographs of the BC-based and BC-DEX/TC-2-based cortical electrodes respectively on the left and right cortical surfaces of a rat brain (left) and fixed with dental cement (right). **i** Comparison of ECoG signals recorded from all nine channels from the BC-based and BC-DEX/TC-2-based cortical electrodes. BC: bacterial cellulose; DEX: dexamethasone; TC: tetracycline; ECoG: electrocorticography

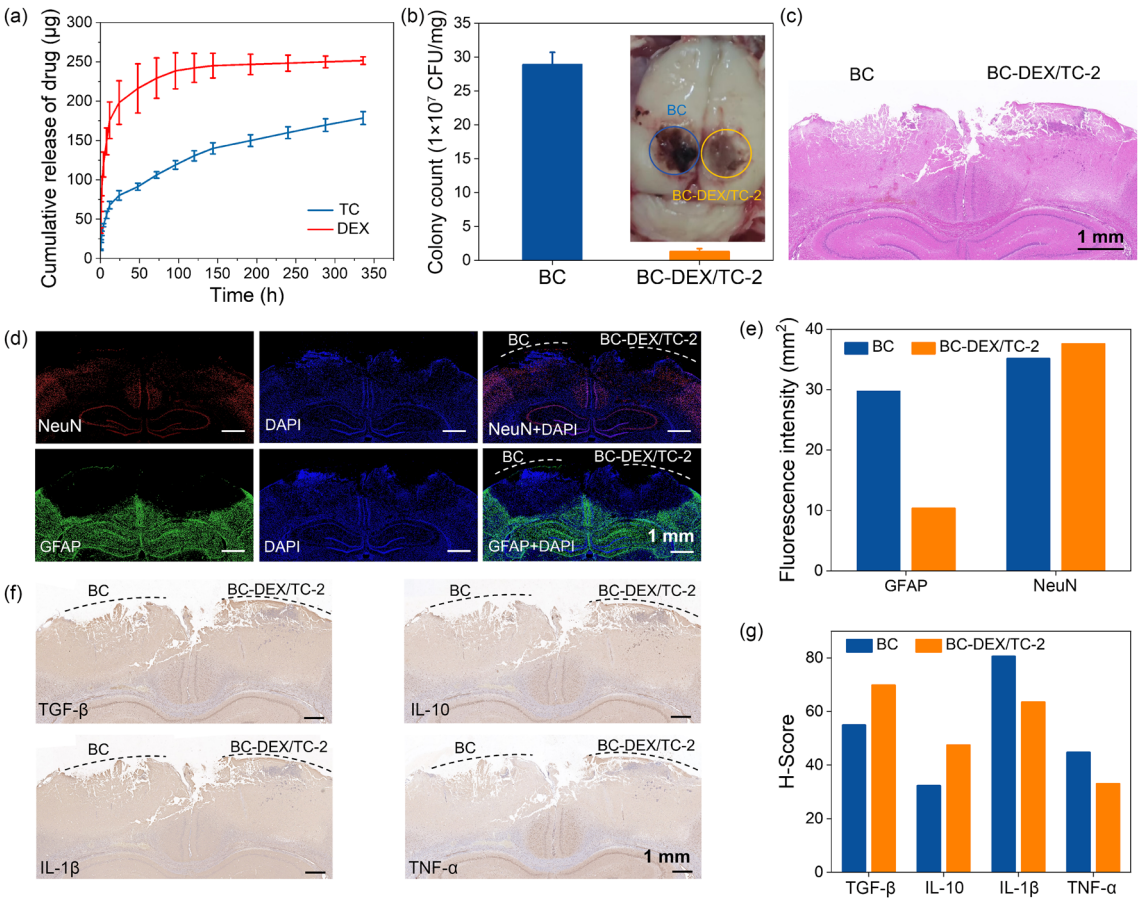

Fig. 6 **a** In vitro cumulative release curve of TC and DEX from BC-DEX/TC-2-based electrodes in ACSF (data are expressed as mean±standard deviation, *n*=5). **b** Colony counts at the interface between brain tissue and BC-based and BC-DEX/TC-2-based electrodes after three days of implantation. The inserted photograph shows brain tissue after implantation of BC-based and BC-DEX/TC-2-based electrodes for three days. Data are expressed as mean±standard deviation, *n*=3–5. **c** H&E staining analysis of brain tissue after three days of BC-based and BC-DEX/TC-2-based electrode implantation. **d** NeuN (red), DAPI (blue), and GFAP (green) immunohistochemistry staining after three days of BC-based and BC-DEX/TC-2-based electrode implantation. White dashed lines indicate the section (position) of the electrodes. **e** Relative fluorescence intensity of neurons and astrocytes in the corresponding brain after three days of implantation of BC-based and BC-DEX/TC-2-based electrodes. **f** Histochemistry of tissue inflammatory factors (i.e., TGF-β, IL-10, IL-1β, and TNF-α) at the interface between brain tissue and BC-based and BC-DEX/TC-2-based electrodes after three days of implantation. **g** H-Score of inflammatory factors. The H-Score is a value between 0 and 300; the higher the value, the stronger the comprehensive positive intensity. TC: tetracycline; DEX: dexamethasone; BC: bacterial cellulose; ACSF: artificial cerebrospinal fluid; H&E: hematoxylin–eosin; NeuN: neuronal nuclei antigen; DAPI: 4′,6-diamidino-2-phenylindole; GFAP: glial fibrillary acidic protein; TGF-β: transforming growth factor-β; IL-10: interleukin-10; IL-1β: interleukin-1β; TNF-α: tumor necrosis factor-α

Supplementary Information The online version contains supplementary material available at https://doi.org/10.1007/s42242-024-00299-x.

Acknowledgements We acknowledge the financial support from the National Natural Science Foundation of China (Nos. 52073230, 62204204, and 62288102), the Shaanxi Provincial Science Fund for Distinguished Young Scholars (No. 2023-JC-JQ-32), the Science and Technology Innovation 2030-Major Project (No. 2022ZD0208601), the Shanghai Sailing Program (No. 21YF1451000), and the China National Postdoctoral Program for Innovative Talents (No. BX20230494).

Author contributions RRQ and TL were involved in investigation, methodology, writing—original draft, formal analysis, and data curation; YFT contributed to investigation, methodology, formal analysis, and data curation; FQS and YHZ contributed to investigation, methodology, and data curation; RHL and XLY were involved in methodology and data curation; BWJ, PL, and WH contributed to conceptualization, methodology, project administration, resources, writing—review and editing, supervision, funding acquisition, and data curation.

Declarations

Conflict of interest The authors declare that they have no conflict of interest.

Ethical approval All animal experimental protocols and handling procedures were approved by the Institutional Animal Care and Use

Committee (IACUC) of Northwestern Polytechnical University, with the ethical number 202301054.

References

1. Rivnay J, Wang HL, Fenno L et al (2017) Next-generation probes, particles, and proteins for neural interfacing. Sci Adv 3(6):e1601649. https://doi.org/10.1126/sciadv.1601649
2. Chiang CH, Won SM, Orsborn AL et al (2020) Development of a neural interface for high-definition, long-term recording in rodents and nonhuman primates. Sci Transl Med 12(538):eaay4682. https://doi.org/10.1126/scitranslmed.aay4682
3. Jiang Y, Ji SB, Sun J et al (2023) A universal interface for plug-and-play assembly of stretchable devices. Nature 614(7948):456–462. https://doi.org/10.1038/s41586-022-05579-z
4. Zhang YC, Zheng N, Cao Y et al (2019) Climbing-inspired twining electrodes using shape memory for peripheral nerve stimulation and recording. Sci Adv 5(4):eaaw1066. https://doi.org/10.1126/sciadv.aaw1066
5. Boyden ES (2023) A history of optogenetics: the development of tools for controlling brain circuits with light. F1000 Biol Rep 3(1):11. https://doi.org/10.3410/B3-11
6. Atherton E, Hu Y, Brown S et al (2022) A 3D in vitro model of the device tissue interface: functional and structural symptoms of innate neuroinflammation are mitigated by antioxidant ceria nanoparticles. J Neur Eng 19(3):036004. https://doi.org/10.1088/1741-2552/ac6908
7. Ahmadabadi HY, Yu K, Kizhakkedathu JN (2020) Surface modification approaches for prevention of implant associated infections. Colloid Surf B Biointerface 193:111116. https://doi.org/10.1016/j.colsurfb.2020.111116
8. Bettinger CJ, Ecker M, Yoshida Kozai TD et al (2020) Recent advances in neural interfaces materials chemistry to clinical translation. MRS Bull 45(8):655–668. https://doi.org/10.1557/mrs.2020.195
9. Minev IR, Musienko P, Hirsch A et al (2015) Electronic dura mater for long-term multimodal neural interfaces. Science 347(6218):159–163. https://doi.org/10.1126/science.1260318
10. Balakrishnan G, Song J, Mou CC et al (2021) Recent progress in materials chemistry to advance flexible bioelectronics in medicine. Adv Mater 34(10):e2106787. https://doi.org/10.1002/adma.202106787
11. Liu LL, Liu YF, Tang RT et al (2022) Stable and low resistance polydopamine methacrylamide polyacrylamide hydrogel for brain computer interface. Sci China Mater 65(8):2298–2308. https://doi.org/10.1007/s40843-022-2145-3
12. Yuk H, Lu BY, Zhao XH (2019) Hydrogel bioelectronics. Chem Soc Rev 48(6):1642–1667. https://doi.org/10.1039/c8cs00595h
13. Zhang DH, Chen Q, Shi C et al (2021) Dealing with the foreign-body response to implanted biomaterials: strategies and applications of new materials. Adv Funct Mater 31(6):2007226. https://doi.org/10.1002/adfm.202170040
14. Gregory DA, Tripathi L, Fricker ATR et al (2021) Bacterial cellulose: a smart biomaterial with diverse applications. Mater Sci Eng R Rep 145:100623. https://doi.org/10.1016/j.mser.2021.100623
15. Liu W, Du HS, Zhang MM et al (2020) Bacterial cellulose based composite scaffolds for biomedical applications: a review. ACS Sustain Chem Eng 8(20):7536–7562. https://doi.org/10.1021/acssuschemeng.0c00125
16. Wahid F, Huang LH, Zhao XQ et al (2021) Bacterial cellulose and its potential for biomedical applications. Biotechnol Adv 53:107856. https://doi.org/10.1016/j.biotechadv.2021.107856
17. Shao W, Liu H, Wang SX et al (2016) Controlled release and antibacterial activity of tetracycline hydrochloride-loaded bacterial cellulose composite membranes. Carbohydr Polym 145:114–120. https://doi.org/10.1016/j.carbpol.2016.02.065
18. Zheng L, Li SS, Luo JW et al (2020) Latest advances on bacterial cellulose based antibacterial materials as wound dressings. Front Bioeng Biotechnol 8:593768. https://doi.org/10.3389/fbioe.2020.593768
19. Zhang YN, Chen YJ, Li X et al (2021) Bacterial cellulose hydrogel: a promising electrolyte for flexible zinc-air batteries. J Power Sour 482:228963. https://doi.org/10.1016/j.jpowsour.2020.228963
20. Pan XS, Li J, Ma N et al (2023) Bacterial cellulose hydrogel for sensors. Chem Eng J 461:142062. https://doi.org/10.1016/j.cej.2023.142062
21. Hu Y, Chen CT, Yang LY et al (2019) Handy purifier based on bacterial cellulose and Ca montmorillonite composites for efficient removal of dyes and antibiotics. Carbohydr Polym 222:115017. https://doi.org/10.1016/j.carbpol.2019.115017
22. Ozseker EE, Akkaya A (2016) Development of a new antibacterial biomaterial by tetracycline immobilization on calcium alginate beads. Carbohydr Polym 151:441–451. https://doi.org/10.1016/j.carbpol.2016.05.073
23. Dang TT, Bratlie KM, Bogatyrev SR et al (2011) Spatiotemporal effects of a controlled release anti inflammatory drug on the cellular dynamics of host response. Biomaterials 32(19):4464–4470. https://doi.org/10.1016/j.biomaterials.2011.02.048
24. Boehler C, Kleber C, Martini N et al (2017) Actively controlled release of dexamethasone from neural microelectrodes in a chronic in vivo study. Biomaterials 129:176–187. https://doi.org/10.1016/j.biomaterials.2017.03.019
25. Liu W, Du H, Zheng T et al (2021) Biomedical applications of bacterial cellulose based composite hydrogels. Curr Med Chem 28(40):8319–8332. https://doi.org/10.2174/0929867328666210412124444
26. Zhang KY, Feng Q, Fang ZW et al (2021) Structurally dynamic hydrogels for biomedical applications: pursuing a fine balance between macroscopic stability and microscopic dynamics. Chem Rev 121(18):11149–11193. https://doi.org/10.1021/acs.chemrev.1c00071
27. Ji BW, Xie ZQ, Hong W et al (2020) Stretchable Parylene-C electrodes enabled by serpentine structures on arbitrary elastomers by silicone rubber adhesive. J Materiomics 6(2):330–338. https://doi.org/10.1016/j.jmat.2019.11.006
28. Ji BW, Guo ZJ, Wang MH et al (2018) Flexible polyimide-based hybrid opto-electric neural interface with 16 channels of micro-LEDs and electrodes. Microsyst Nanoeng 4(1):27. https://doi.org/10.1038/s41378-018-0027-0